Spin Ordering and Thermodynamical Properties in Spin-Pair Systems under Magnetic Fields

Masashi TACHIKI and Takemi YAMADA

The Research Institute for Iron, Steel and Other Metals
Tohoku University, Sendai

(Received, November 10 1970)

It has recently been shown that in spin-pair systems a new type of spin ordering occurs under magnetic fields. In the present paper, the spin ordering in general cases of the inter-pair exchange interaction and the thermodynamical properties of these systems are investigated on the basis of molecular field theory. Various types of spin ordering appear depending on the strength of the inter-pair exchange interaction and the external magnetic field. The specific heat originating from the short range order of spins in a one-dimensional lattice is also calculated for a purpose of comparison with experiments in $Cu(NO_3)_2\,2.5\,H_2O$.

§1. Introduction

In $Cu(NO_3)_2 2.5 H_2O$, the Cu^{2+} ions are coupled in pairs by isotropic antiferromagnetic exchange and the pairs are also coupled by weak antiferromagnetic exchange. The ground state of the pair is a singlet, separated by about 5.2°K from an excited triplet. In an external magnetic field the triplet splits and the lowest component of the triplet approaches the singlet as the field increases. Both the two levels cross at about $H=36$ kOe.[1)~3)]

Recently Haseda et al.[4)] have made an experiment of cooling by adiabatic magnetization using this crystal and have observed that when cooling begins below 0.7°K the temperature versus magnetic field curves become flat or slightly convex between 30 kOe and 48 kOe, as shown in Fig. 1. We have considered that this anomaly in the field dependence of temperature corresponds to occurrence of a new type of spin ordering, and have suggested the following mechanism for this ordering.[5)] The inter-pair exchange interaction has non-vanishing matrix elements between the singlet and triplet states, and the interaction causes a mixing between them. Although the inter-pair exchange interaction is weaker than the intra-pair exchange interaction, the mixing due to the inter-pair exchange interaction cannot be neglected near the point of level crossing. If the isotropic inter-pair exchange interaction is projected onto the subspace spanned by the singlet and the lowest component of the triplet, the interaction becomes anisotropic with respect to the direction of the applied magnetic field; the component of the exchange interaction perpendicular to the field becomes larger than the component parallel to the field. Furthermore,

Downloaded from https://academic.oup.com/ptps/article/doi/10.1143/PTPS.46.291/1875345 by guest on 20 August 2022

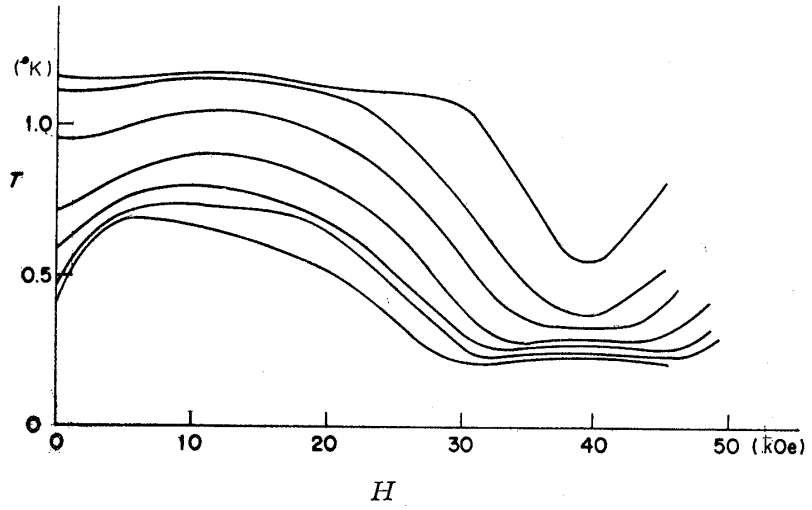

Fig. 1. The field dependence of temperature of $Cu(NO_3)_2 2.5 H_2O$ (powder sample) in adiabatic magnetization process, observed by Haseda et al.[4]

the effective field in this subspace becomes very small near the point of level crossing. As a result, we expect an ordering of the spin component perpendicular to the field in the vicinity of the level crossing at sufficiently low temperatures. On the basis of this model, we calculated the entropy of the system and obtained temperature in adiabatic magnetization process. The field dependence of temperature explains qualitatively the anomaly mentioned above.[5),6)]

After that, Bonner et al.[7)] have proposed two kinds of one-dimensional model for the spin-array in $Cu(NO_3)_2 2.5 H_2O$. Since the arrays of spin-pairs in these models are one-dimensional, no long range order of spins occurs in these systems. However, it has been shown that a short range order which has a similar nature to that of the long range order mentioned above appears in the vicinity of the point of level crossing at sufficiently low temperatures.[8)] It has further been shown that the observed anomaly in the field dependence of temperature is also explained as occurrence of the short range order.[7),8)] One of the aim of the present paper is to calculate the specific heat of spins in the one- and three-dimensional lattices and to show that measurements of the specific heat of $Cu(NO_3)_2 2.5 H_2O$ under magnetic fields may give a possibility to determine whether the anomaly originates from the short range order or from the long range order of spins in this crystal.

So far, we discussed on the case of $Cu(NO_3)_2 2.5 H_2O$. In general cases of the inter-pair exchange interaction, various types of spin ordering under magnetic fields are expected depending on the strength of the interactions. The physical model in this case is described in detail in §2 and the possible types of spin ordering at finite temperatures are discussed in §3. The thermodynamical properties associated with the spin ordering are obtained in §4. For the sake of comparison with experiments, the specific heat originating from the short range order in one-dimensional lattice is calculated in §5.

Downloaded from https://academic.oup.com/ptps/article/doi/10.1143/PTPS.46.291/1875345 by guest on 20 August 2022

§2. Physical model

The Hamiltonian for isolated pairs in an external magnetic field is written as

$$\mathcal{H}_0 = J\sum_i \boldsymbol{s}_{i1}\cdot\boldsymbol{s}_{i2} + g\mu_B \boldsymbol{H}\cdot\sum_i(\boldsymbol{s}_{i1}+\boldsymbol{s}_{i2}), \tag{1}$$

where $\boldsymbol{s}_{i1}$ and $\boldsymbol{s}_{i2}$ are the spins of 1/2 in the i-th pair. In the Hamiltonian (1), the g-factor and the exchange integral are assumed to be isotropic. For the inter-pair exchange interaction, we consider the following general form

$$\mathcal{H}_1 = \sum_{<i,j>}(J_{11}\boldsymbol{s}_{i1}\cdot\boldsymbol{s}_{j1} + J_{22}\boldsymbol{s}_{i2}\cdot\boldsymbol{s}_{j2} + J_{12}\boldsymbol{s}_{i1}\cdot\boldsymbol{s}_{j2} + J_{21}\boldsymbol{s}_{i2}\cdot\boldsymbol{s}_{j1}). \tag{2}$$

In this expression, J_{11} etc. stand for $J_{11}\epsilon_{ij}^{11}$ etc., where $\epsilon_{ij}^{mn}=1$ for the i-j pair interacting with the exchange constant J_{mn}, and $\epsilon_{ij}^{mn}=0$ for the other pairs. Introducing operators $\boldsymbol{S}_i$ and $\boldsymbol{t}_i$ defined by

$$\boldsymbol{S}_i = \boldsymbol{s}_{i1}+\boldsymbol{s}_{i2} \quad \text{and} \quad \boldsymbol{t}_i = \boldsymbol{s}_{i1}-\boldsymbol{s}_{i2}, \tag{3}$$

we write the Hamiltonians (1) and (2) as

$$\mathcal{H}_0 = (J/2)\sum_i \boldsymbol{S}_i^2 + g\mu_B\boldsymbol{H}\cdot\sum_i \boldsymbol{S}_i \tag{4}$$

and

$$\begin{aligned}\mathcal{H}_1 = (1/4)\sum_{<i,j>}[&(J_{11}+J_{22}+J_{12}+J_{21})\boldsymbol{S}_i\cdot\boldsymbol{S}_j \\ &+(J_{11}+J_{22}-J_{12}-J_{21})\boldsymbol{t}_i\cdot\boldsymbol{t}_j+(J_{11}-J_{22}-J_{12}+J_{21})\boldsymbol{S}_i\cdot\boldsymbol{t}_j \\ &+(J_{11}-J_{22}+J_{12}-J_{21})\boldsymbol{t}_i\cdot\boldsymbol{S}_j].\end{aligned} \tag{5}$$

In Eq. (4), a constant term was neglected.

The energy levels of the pair are shown in Fig. 2, where the energy levels are indicated by the eigenvalues of S and S_z. The operator $\boldsymbol{S}$ defined by Eq. (3) has nonvanishing matrix elements only within the same spin multiplets and $\boldsymbol{t}$ has those only between different multiplets. In the following, we neglect the highest two levels of the triplet, and confine ourselves to the subspace spanned by $|0,0\rangle$ and $|1,-1\rangle$. In this case it is con-

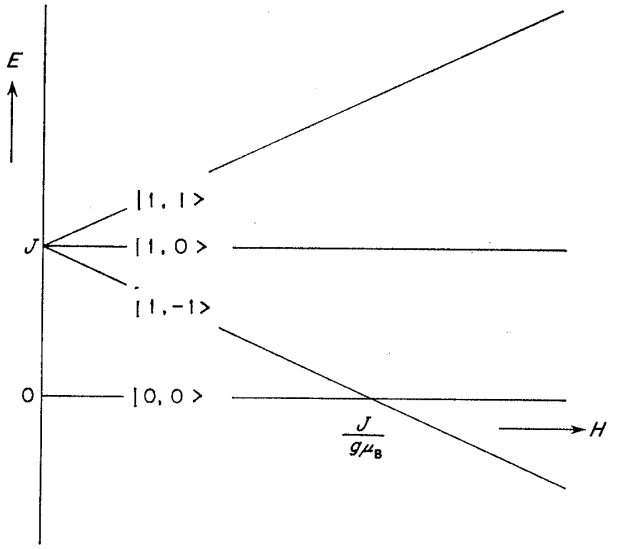

Fig. 2. Energy levels of the spin-pair under a magnetic field.

Downloaded from https://academic.oup.com/ptps/article/doi/10.1143/PTPS.46.291/1875345 by guest on 20 August 2022

venient to rewrite the Hamiltonian using the Pauli spin matrices. Let the states $|0,0\rangle$ and $|1,-1\rangle$ correspond to the states of $\sigma_z=1$ and -1, respectively. Then, $\boldsymbol{S}_i$ and $\boldsymbol{t}_i$ relate to the Pauli spins in the following way:

$$\begin{aligned} &\boldsymbol{S}_i^2=1-\sigma_{zi}, && S_{xi}=S_{yi}=0, \\ &S_{zi}=(1/2)(\sigma_{zi}-1), && t_{xi}=(1/\sqrt{2})\sigma_{xi}, \\ &t_{yi}=(1/\sqrt{2})\sigma_{yi}, && t_{zi}=0. \end{aligned} \tag{6}$$

With use of the relation (6), the total Hamiltonian is written as

$$\begin{aligned} \mathcal{H}&=\mathcal{H}_0+\mathcal{H}_1 \\ &=(N/2)\{J+(\alpha/4)-g\mu_B H\} \\ &\quad+(1/2)\{g\mu_B H-J-(\alpha/2)\}\sum_i \sigma_{zi} \\ &\quad+(1/4)\sum_{<i,j>}[(1/2)(J_{11}+J_{22}-J_{12}-J_{21})(\sigma_{xi}\sigma_{xj}+\sigma_{yi}\sigma_{yj}) \\ &\quad+(1/4)(J_{11}+J_{22}+J_{12}+J_{21})\sigma_{zi}\sigma_{zj}], \end{aligned} \tag{7}$$

where

$$\alpha=(1/4)(J_{11}z_{11}+J_{22}z_{22}+J_{12}z_{12}+J_{21}z_{21}). \tag{8}$$

In Eq. (8), z_{mn} represents the number of neighbors interacting with the exchange constant J_{mn}. The Hamiltonian (8) represents a spin system coupled by an anisotropic exchange interaction in an effective magnetic field $H_{\text{eff}}=H-(1/g\mu_B)\{J+(\alpha/2)\}$.

§3. Spin ordering

In obtaining the solutions for the Hamiltonian (7), we use a two sublattice model and a molecular field approximation. The Hamiltonians for σ and σ' in these sublattices are derived from Eq. (7) as

$$\begin{aligned} \mathcal{H}&=-(1/2)\{f+(\alpha/4)\}+(1/2)f\sigma_z \\ &\quad+(1/4)\{\beta(\langle\sigma_x'\rangle\sigma_x+\langle\sigma_y'\rangle\sigma_y)+\alpha\langle\sigma_z'\rangle\sigma_z\}, \end{aligned} \tag{9}$$

$$\begin{aligned} \mathcal{H}'&=-(1/2)\{f+(\alpha/4)\}+(1/2)f\sigma_z' \\ &\quad+(1/4)\{\beta(\langle\sigma_x\rangle\sigma_x'+\langle\sigma_y\rangle\sigma_y')+\alpha\langle\sigma_z\rangle\sigma_z'\}, \end{aligned} \tag{10}$$

where

$$f=g\mu_B H-J-(\alpha/2), \tag{11}$$

$$\beta=(1/2)(J_{11}z_{11}+J_{22}z_{22}-J_{12}z_{12}-J_{21}z_{21}). \tag{12}$$

In Eqs. (9) and (10), $\langle A\rangle$ indicates the thermal average of A. The eigenvalues of the Hamiltonians (9) and (10) are calculated as

Downloaded from https://academic.oup.com/ptps/article/doi/10.1143/PTPS.46.291/1875345 by guest on 20 August 2022

$$E^{\pm}=-(1/2)\{f+(\alpha/4)\}$$
$$\pm(1/2)\sqrt{\{f+(\alpha/2)\langle\sigma_z\rangle\}^2+\{(\beta/2)\langle\tau'\rangle\}^2}, \tag{13}$$
$$E'^{\pm}=-(1/2)\{f+(\alpha/4)\}$$
$$\pm(1/2)\sqrt{\{f+(\alpha/2)\langle\sigma_z\rangle\}^2+\{(\beta/2)\langle\tau\rangle\}^2}, \tag{14}$$

where $\langle\tau\rangle$ and $\langle\tau'\rangle$ are defined by

$$\langle\boldsymbol{\sigma}\rangle=\langle\sigma_z\rangle(\boldsymbol{H}/|H|)+\langle\tau\rangle\boldsymbol{i}, \tag{15}$$
$$\langle\boldsymbol{\sigma}'\rangle=\langle\sigma_z'\rangle(\boldsymbol{H}/|H|)+\langle\tau'\rangle\boldsymbol{i}', \tag{16}$$

$\boldsymbol{i}$ and $\boldsymbol{i}'$ being unit vectors perpendicular to the external field. The Helmholtz free energy is written as

$$F=N[-(kT/2)(\ln Z+\ln Z')$$
$$-(\alpha/8)\langle\sigma_z\rangle\langle\sigma_z'\rangle-(\beta/8)\langle\tau\rangle\langle\tau'\rangle\cos\varphi], \tag{17}$$

where

$$Z=\exp(-E^{+}/kT)+\exp(-E^{-}/kT), \tag{18}$$
$$Z'=\exp(-E'^{+}/kT)+\exp(-E'^{-}/kT), \tag{19}$$
$$\cos\varphi=\boldsymbol{i}\cdot\boldsymbol{i}'. \tag{20}$$

The last two terms in Eq. (17) were subtracted from $-(NkT/2)(\ln Z+\ln Z')$, since twice the inter-pair exchange energy is included in $-(NkT/2)(\ln Z+\ln Z')$. By using Eqs. (13) and (14), the free energy (17) is calculated as

$$F=N[-kT\ln 2-(1/2)\{f+(\alpha/4)\}$$
$$-(kT/2)\{\ln\cosh x+\ln\cosh x'\}$$
$$-(\alpha/8)\langle\sigma_z\rangle\langle\sigma_z'\rangle-(\beta/8)\langle\tau\rangle\langle\tau'\rangle\cos\varphi], \tag{21}$$

with

$$x=(2kT)^{-1}\sqrt{\{f+(\alpha/2)\langle\sigma_z\rangle\}^2+\{(\beta/2)\langle\tau\rangle\}^2}, \tag{22}$$
$$x'=(2kT)^{-1}\sqrt{\{f+(\alpha/2)\langle\sigma_z'\rangle\}^2+\{(\beta/2)\langle\tau'\rangle\}^2}. \tag{23}$$

The values of $\langle\sigma_z\rangle$, $\langle\tau\rangle$, $\langle\sigma_z'\rangle$, $\langle\tau'\rangle$ and φ are determined by minimizing the free energy (21) with respect to them. From the conditions $\partial F/\partial\langle\sigma_z\rangle=0$, $\partial F/\partial\langle\tau\rangle=0$ etc., we have the following equations

$$(\tanh x/x)\{f+(\alpha/2)\langle\sigma_z\rangle\}/(2kT)=-\langle\sigma_z'\rangle, \tag{24}$$
$$(\tanh x'/x')\{f+(\alpha/2)\langle\sigma_z'\rangle\}/(2kT)=-\langle\sigma_z\rangle, \tag{25}$$
$$(\tanh x/x)\{(\beta/2)\langle\tau\rangle\}/(2kT)=-\langle\tau'\rangle\cos\varphi, \tag{26}$$
$$(\tanh x'/x')\{(\beta/2)\langle\tau'\rangle\}/(2kT)=-\langle\tau\rangle\cos\varphi, \tag{27}$$
$$\beta\sin\varphi\langle\tau\rangle\langle\tau'\rangle=0. \tag{28}$$

Downloaded from https://academic.oup.com/ptps/article/doi/10.1143/PTPS.46.291/1875345 by guest on 20 August 2022

Equation (28) shows that

$$\varphi=0 \text{ or } \pi \qquad \text{when} \quad \beta\langle\tau\rangle\langle\tau'\rangle\neq 0. \tag{29}$$

Equations (26) and (27) have two types of the solution

$$\langle\tau\rangle=\langle\tau'\rangle=0 \tag{30}$$

and

$$\langle\tau\rangle\neq 0, \qquad \langle\tau'\rangle\neq 0. \tag{31}$$

Inspecting Eqs. (29), (26) and (27), we see that the solution of the type (31) is possible only when

$$\begin{aligned} &\cos\varphi=-1 \qquad \text{for positive } \beta, \\ &\cos\varphi=+1 \qquad \text{for negative } \beta. \end{aligned} \tag{32}$$

For solutions of the type (31), we assume

$$\langle\tau\rangle=\langle\tau'\rangle. \tag{33}$$

We first consider the solution of the type (30). Inserting Eq. (30) into Eqs. (22) and (23), we have

$$x=(2kT)^{-1}|f+(\alpha/2)\langle\sigma_z\rangle|, \tag{34}$$

$$x'=(2kT)^{-1}|f+(\alpha/2)\langle\sigma_z'\rangle|. \tag{35}$$

In this case, we can rewrite Eqs. (24), (25), (34) and (35) as

$$\tanh y=-\langle\sigma_z'\rangle, \tag{36}$$

$$\tanh y'=-\langle\sigma_z\rangle, \tag{37}$$

$$y=(2kT)^{-1}\{f+(\alpha/2)\langle\sigma_z\rangle\}, \tag{38}$$

$$y'=(2kT)^{-1}\{f+(\alpha/2)\langle\sigma_z'\rangle\}. \tag{39}$$

Combining these equations, we have a simultaneous equation

$$\tanh y=-(4kT/\alpha)y'+(2f/\alpha), \tag{40·1}$$

$$\tanh y'=-(4kT/\alpha)y+(2f/\alpha). \tag{40·2}$$

When α is positive, Eq. (40) has the following two types of solution

$$(i) \qquad \tanh y=\tanh y', \tag{41}$$

$$(ii) \qquad \tanh y\neq\tanh y'. \tag{42}$$

When α is negative, Eq. (40) has only the solution of type (41). The values of $\langle\sigma_z\rangle$ and $\langle\sigma_z'\rangle$, obtained from Eqs. (36), (37) and (40), are shown in Fig. 3 as functions of temperature and magnetic field.

Downloaded from https://academic.oup.com/ptps/article/doi/10.1143/PTPS.46.291/1875345 by guest on 20 August 2022

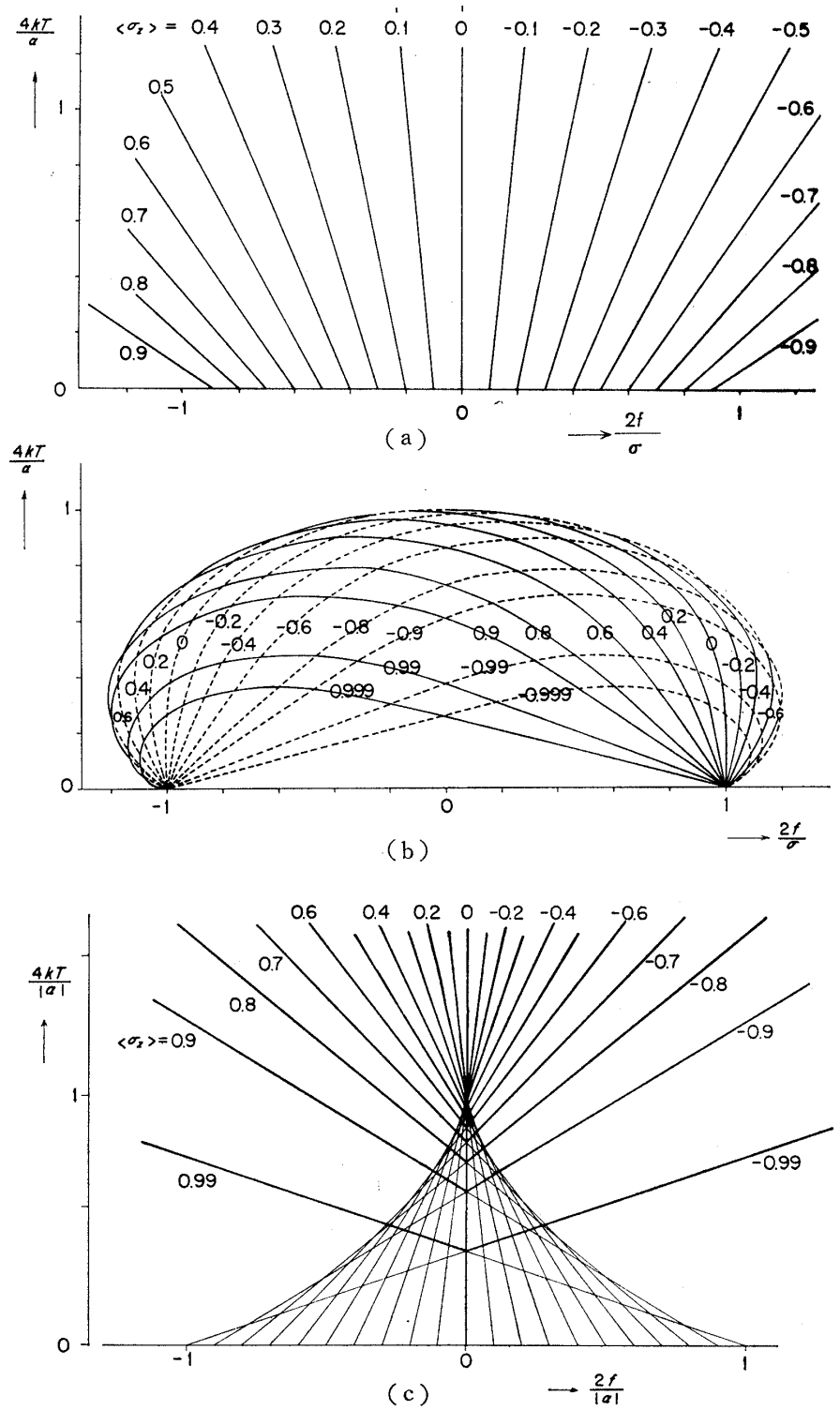

Fig. 3. The values of $\langle\sigma_z\rangle$ and $\langle\sigma'_z\rangle$ obtained from Eqs. (36), (37) and (40).

(a) The solution of type (i) ($\langle\sigma_z\rangle=\langle\sigma'_z\rangle$) in the case of $\alpha>0$.

(b) The solution of type (ii) in the case of $\alpha>0$. Solid and dashed lines correspond to $\langle\sigma_z\rangle$ and $\langle\sigma'_z\rangle$, respectively.

(c) The solution in the case of $\alpha<0$. The solution is a triple-valued function of T and f in the region surrounded by the envelope of thin lines. Thick lines correspond to the solution of the lowest free energy.

Downloaded from https://academic.oup.com/ptps/article/doi/10.1143/PTPS.46.291/1875345 by guest on 20 August 2022

Next we consider the solution of the type

$$\langle\tau\rangle=\langle\tau'\rangle\neq 0. \tag{43}$$

Inserting Eqs. (32) and (43) into Eqs. (26) and (27), we have

$$\tanh x/x=\tanh x'/x'=4kT/|\beta|. \tag{44}$$

The values of $\langle\sigma_z\rangle$ and $\langle\sigma_z'\rangle$ are determined from Eqs. (24), (25) and (44) as

$$\langle\sigma_z\rangle=\langle\sigma_z'\rangle=-2f/(\alpha+|\beta|). \tag{45}$$

These values are independent of temperature. The value of $\langle\tau\rangle$ is determined from Eqs. (22), (44) and (45) as

$$\langle\tau\rangle=\sqrt{\tanh^2 x-\{2f/(\alpha+|\beta|)\}^2}, \tag{46}$$

where $\tanh x$ is the solution of Eq. (44). The value of $\tanh x(=\sqrt{\langle\sigma_z\rangle^2+\langle\tau\rangle^2})$ is independent of magnetic field. In Fig. 4, the values of $\langle\sigma_z\rangle$ and $\langle\tau\rangle$ are plotted as functions of temperature and magnetic field.

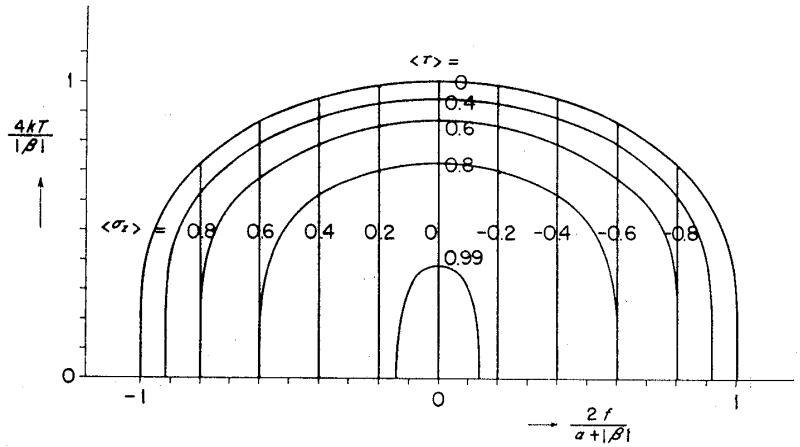

Fig. 4. The values of $\langle\sigma_z\rangle$ and $\langle\tau\rangle$ obtained from Eqs. (44), (45) and (46). The figure corresponds to the case of $\alpha+|\beta|>0$.

The above results are summarized as follows: We have the following three phases.

Phase (i).

$$\left.\begin{aligned}&\langle\sigma_z\rangle=\langle\sigma_z'\rangle=-\tanh y,\\&\tanh y=-(4kT/\alpha)y+(2f/\alpha),\\&\langle\tau\rangle=\langle\tau'\rangle=0,\end{aligned}\right\} \tag{47}$$

$$F^{(i)}=N[-kT\ln 2-(1/2)\{f+(\alpha/4)\}-kT\ln\cosh y-(\alpha/8)\tanh^2 y]. \tag{48}$$

Downloaded from https://academic.oup.com/ptps/article/doi/10.1143/PTPS.46.291/1875345 by guest on 20 August 2022

The real spins $\langle \boldsymbol{s}_1 \rangle$, $\langle \boldsymbol{s}_2 \rangle$, $\langle \boldsymbol{s}_1' \rangle$ and $\langle \boldsymbol{s}_2' \rangle$ are all parallel and have the same magnitude

$$\langle \boldsymbol{s}_1 \rangle = \langle \boldsymbol{s}_2 \rangle = \langle \boldsymbol{s}_1' \rangle = \langle \boldsymbol{s}_2' \rangle = (1/4)(\langle \sigma_z \rangle - 1)(\boldsymbol{H}/|H|). \tag{49}$$

Phase (ii). This phase is possible only when $\alpha > 0$.

$$\left.\begin{aligned} &\langle \sigma_z \rangle = -\tanh y', \\ &\langle \sigma_z' \rangle = -\tanh y. \end{aligned}\right\} \tag{50}$$

The values of $\tanh y$ and $\tanh y'$ are obtained from Eq. (40).

$$\langle \tau \rangle = \langle \tau' \rangle = 0.$$

$$\begin{aligned} F^{(ii)} = N[&-kT\ln 2 - (1/2)\{f + (\alpha/4)\} \\ &- (kT/2)(\ln\cosh y + \ln\cosh y') \\ &- (\alpha/8)\tanh y \tanh y']. \end{aligned} \tag{51}$$

The real spins are given by

$$\begin{aligned} &\langle \boldsymbol{s}_1 \rangle = \langle \boldsymbol{s}_2 \rangle = (1/4)(\langle \sigma_z \rangle - 1)(\boldsymbol{H}/|H|), \\ &\langle \boldsymbol{s}_1' \rangle = \langle \boldsymbol{s}_2' \rangle = (1/4)(\langle \sigma_z' \rangle - 1)(\boldsymbol{H}/|H|). \end{aligned} \tag{52}$$

Phase (iii).

$$\begin{aligned} &\langle \sigma_z \rangle = \langle \sigma_z' \rangle = -2f/(\alpha + |\beta|), \\ &\langle \tau \rangle = \langle \tau' \rangle = \sqrt{\tanh^2 x - \{2f/(\alpha + |\beta|)\}^2}. \end{aligned} \tag{53}$$

The value of $\tanh x$ is obtained from Eq. (44).

$$\begin{aligned} F^{(iii)} = N[&-kT\ln 2 - (1/2)\{f + (\alpha/4)\} \\ &- kT\ln\cosh x + (|\beta|/8)\tanh^2 x - f^2/\{2(\alpha + |\beta|)\}]. \end{aligned} \tag{54}$$

The real spins are given by

$$\left.\begin{aligned} &\langle \boldsymbol{s}_1 \rangle = (1/4)(\langle \sigma_z \rangle - 1)(\boldsymbol{H}/|H|) + (1/2\sqrt{2})\langle \tau \rangle \boldsymbol{i}, \\ &\langle \boldsymbol{s}_2 \rangle = (1/4)(\langle \sigma_z \rangle - 1)(\boldsymbol{H}/|H|) - (1/2\sqrt{2})\langle \tau \rangle \boldsymbol{i}, \\ &\langle \boldsymbol{s}_1' \rangle = (1/4)(\langle \sigma_z \rangle - 1)(\boldsymbol{H}/|H|) + (1/2\sqrt{2})\langle \tau \rangle \boldsymbol{i}', \\ &\langle \boldsymbol{s}_2' \rangle = (1/4)(\langle \sigma_z \rangle - 1)(\boldsymbol{H}/|H|) - (1/2\sqrt{2})\langle \tau \rangle \boldsymbol{i}', \end{aligned}\right\} \tag{55}$$

where $\boldsymbol{i} = \pm \boldsymbol{i}'$ according as $\beta \lessgtr 0$.

Comparing the free energies in these phases, we obtain phase diagrams in the H–T plane. The phase diagrams are characterized by the ratio of the exchange constants α and β.

Downloaded from https://academic.oup.com/ptps/article/doi/10.1143/PTPS.46.291/1875345 by guest on 20 August 2022

Case *a*. When $\alpha > |\beta|$, all the three phases appear as shown in Fig. 5(a) (The figure corresponds to the case of $\alpha = 2|\beta|$). The transition between Phases (ii) and (iii) is of the first order and those between Phases (i) and (ii) and Phases (i) and (iii) are of the second order. Spin configurations at typical points in the H–T plane are also shown in the figure. In Phase (i), all the spin polarizations are along the field and their magnitudes are the same. In Phase (ii), the spin polarizations are also along the field but their magnitudes in the two sublattices are different. In Phase (iii), the spin components perpendicular to the field appear.

Case *b*. When $|\alpha| < |\beta|$, Phases (i) and (iii) appear as shown in Fig. 5(b). The transition between them is of the second order. The spin configurations in the case of $\beta > 0$ are also shown in the figure. In the case of $\beta < 0$, the

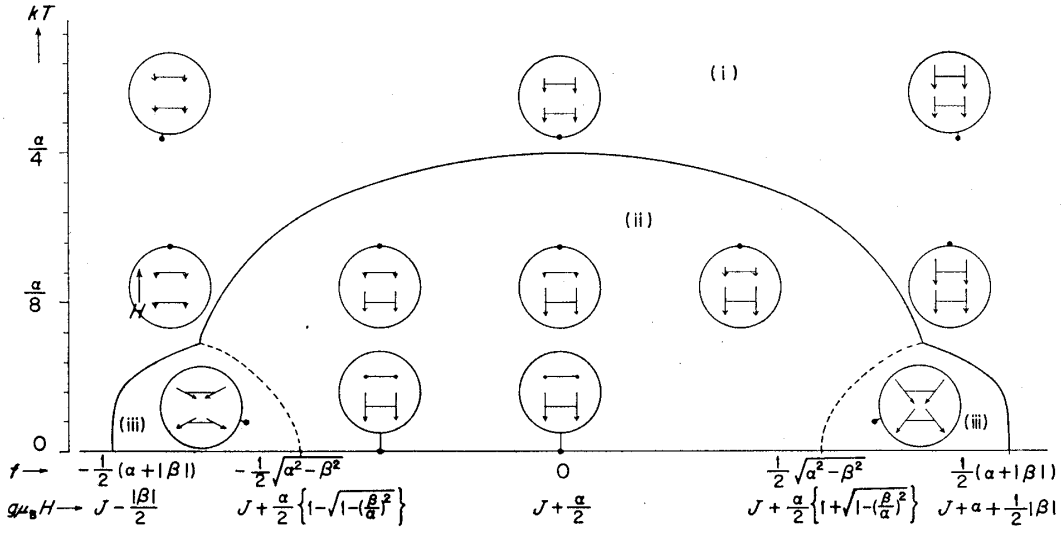

(a)

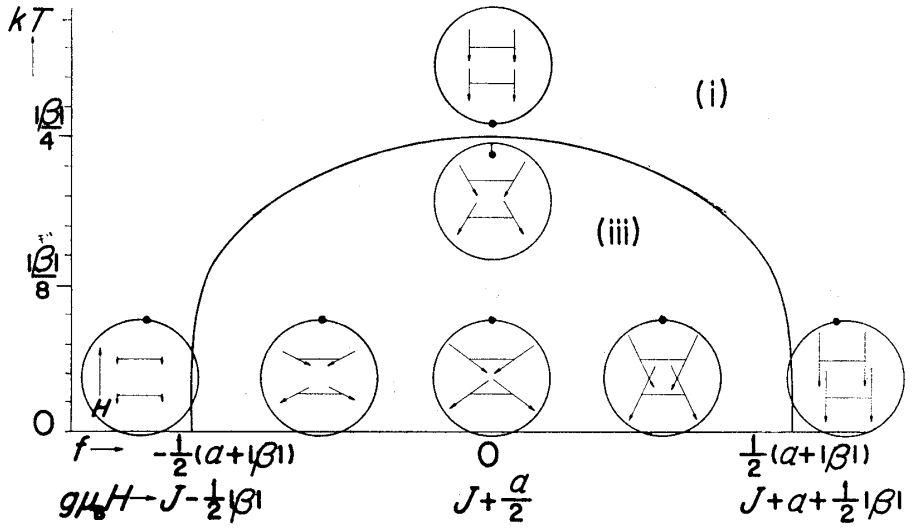

(b)

Downloaded from https://academic.oup.com/ptps/article/doi/10.1143/PTPS.46.291/1875345 by guest on 20 August 2022

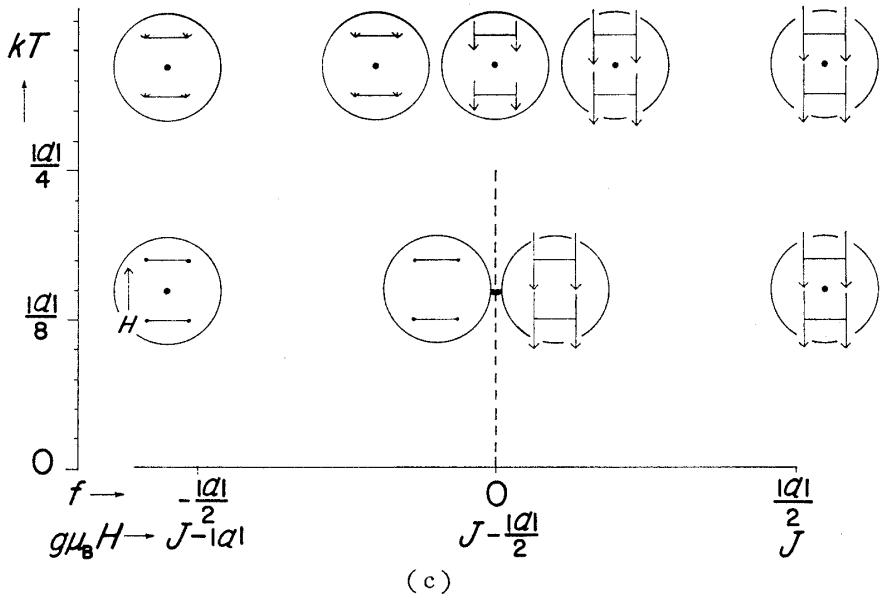

Fig. 5. Phase diagrams and spin configurations at typical points in the H-T plane. Phase boundaries indicated by dotted and solid lines correspond to the first and second order transitions, respectively. The spin configuration at the point indicated by spot is shown in the circle near the spot. The connected arrows represent the spins in a pair.

(a) Case a: $\alpha>|\beta|$. The figure corresponds to the case of $\alpha=2|\beta|$.
(b) Case b: $|\alpha|<|\beta|$. The spin configuration corresponds to the case of positive β.
(c) Case c: $\alpha<0$, $|\alpha|>|\beta|$.

perpendicular components of spins in one sublattice become parallel to the corresponding ones in the other sublattice in Phase (iii).

Case c. When $\alpha<0$ and $|\alpha|>|\beta|$, only Phase (i) appears. The solution of Eq. (47) in this case is a triple-valued function of H and T (Fig. 3(c)). A first order transition with respect to the field occurs at $f=0$ at temperatures below $|\alpha|/4k$ as shown by a dotted line in Fig. 5(c). Typical spin configurations are also shown in Fig. 5(c).

§4. Thermodynamical properties

Magnetization M, entropy S and specific heat at constant field C_H are obtained, by using usual thermodynamical relations and the conditions $\partial F/\partial\langle\sigma_z\rangle=0$ etc., as follows:

For Phase (i),

$$M^{(i)}=(Ng\mu_B/2)(1+\tanh y), \tag{56}$$

$$S^{(i)}=Nk(\ln 2+\ln\cosh y-y\tanh y), \tag{57}$$

$$C_H^{(i)}=Nky^2\{\cosh^2 y+(\alpha/4kT)\}^{-1}. \tag{58}$$

Downloaded from https://academic.oup.com/ptps/article/doi/10.1143/PTPS.46.291/1875345 by guest on 20 August 2022

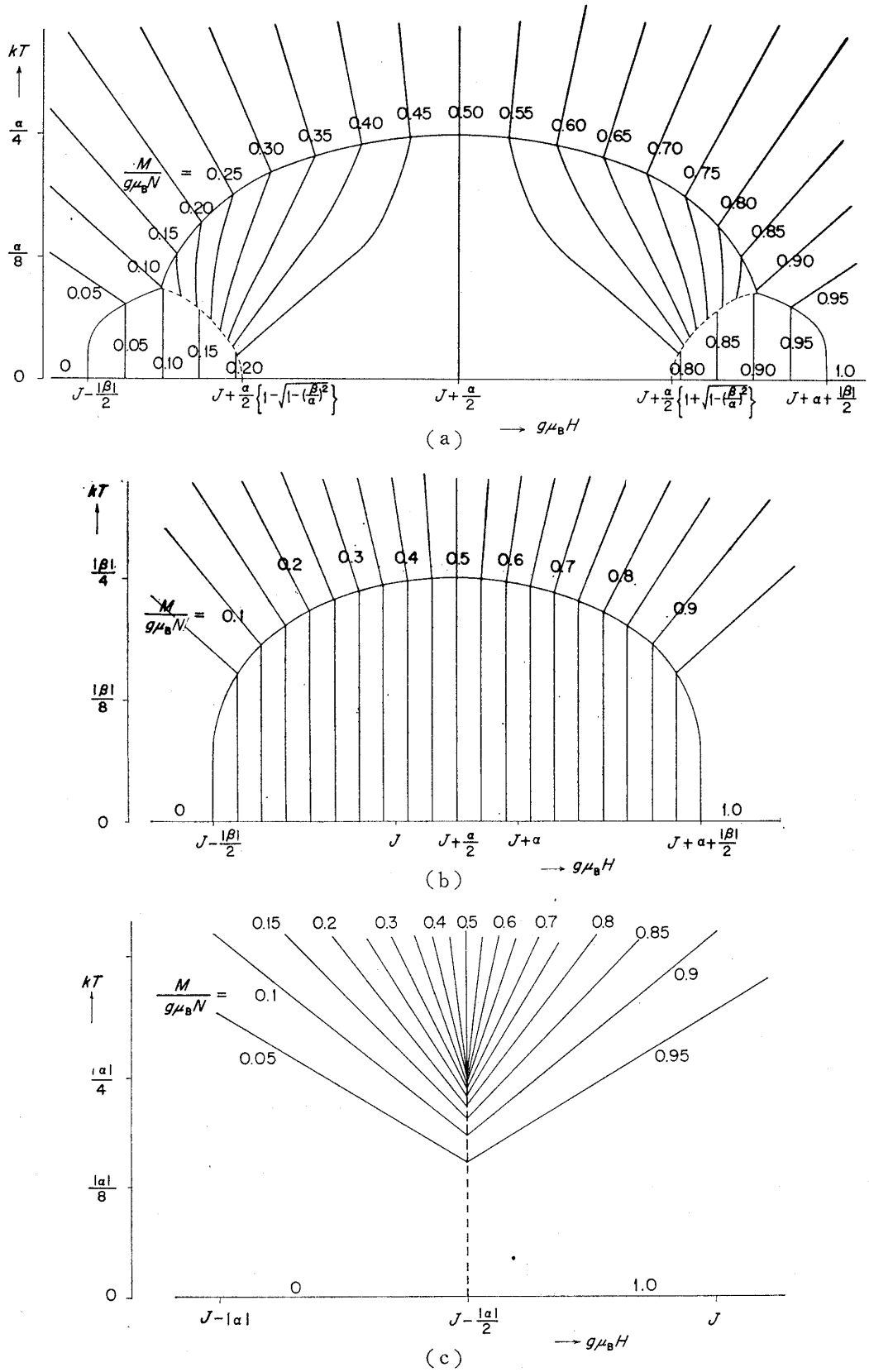

Fig. 6. The contour lines of constant magnetization in the H-T plane. (a) Case a, (b) Case b, (c) Case c.

Downloaded from https://academic.oup.com/ptps/article/doi/10.1143/PTPS.46.291/1875345 by guest on 20 August 2022

For Phase (ii),

$$M^{(ii)}=(Ng\mu_B/2)\{1+(1/2)(\tanh y+\tanh y')\}, \tag{59}$$

$$S^{(ii)}=Nk\{\ln 2+(1/2)(\ln\cosh y+\ln\cosh y') -(1/2)(y\tanh y+y'\tanh y')\}, \tag{60}$$

$$C_H^{(ii)}=Nk(2kT/\alpha) \times\{2yy'-(4kT/\alpha)(y^2\cosh^2 y'+y'^2\cosh^2 y)\} \times\{1-(4kT/\alpha)^2\cosh^2 y\cosh^2 y'\}^{-1}. \tag{61}$$

For Phase (iii),

$$M^{(iii)}=(Ng\mu_B/2)\{1+2f/(\alpha+|\beta|)\}, \tag{62}$$

$$S^{(iii)}=Nk(\ln 2+\ln\cosh x-x\tanh x), \tag{63}$$

$$C_H^{(iii)}=Nkx^2\{\cosh^2 x-|\beta|/4kT\}^{-1}. \tag{64}$$

The quantities y, y', and x have been determined as functions of H and T. In Fig. 6, the contour lines of constant magnetization in the H–T plane are shown for Cases a, b and c. We see in the figure that the isothermal magnetization at low temperatures depends strongly on the ratio of the exchange constants α and β.

In Fig. 7, the contour lines of constant entropy in the H–T plane are shown for Cases a, b and c. In adiabatic process, the spin temperature changes as a function of H along the line of constant entropy. When the line of constant entropy is cut by a phase boundary of the first order transition (the lines of $S/Nk=0.1$, 0.2 and 0.3 in Fig. 7(a)), the temperature versus field curves exhibit a hysteresis, as shown in Fig. 7(a).

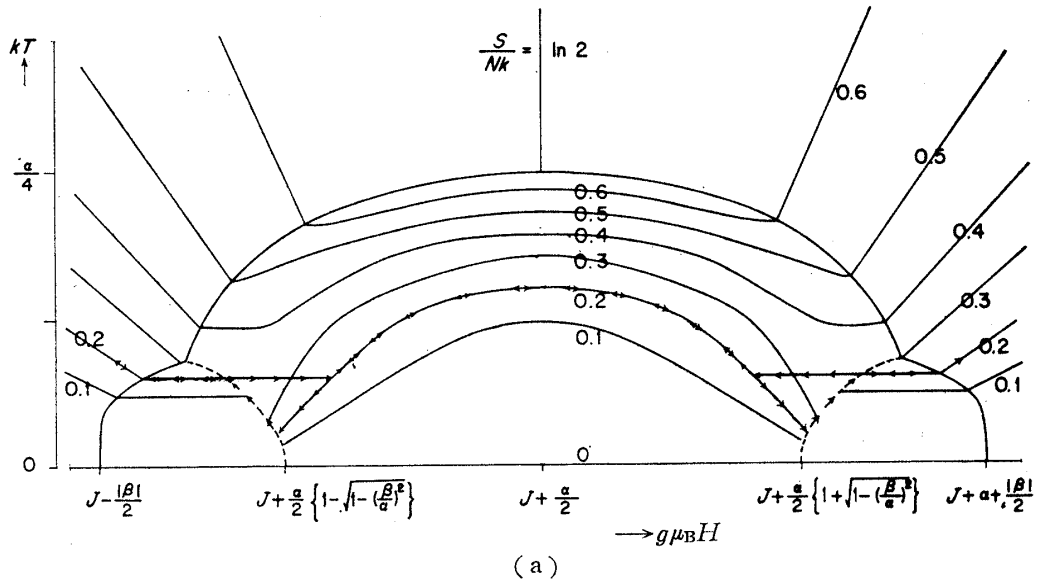

(a)

Downloaded from https://academic.oup.com/ptps/article/doi/10.1143/PTPS.46.291/1875345 by guest on 20 August 2022

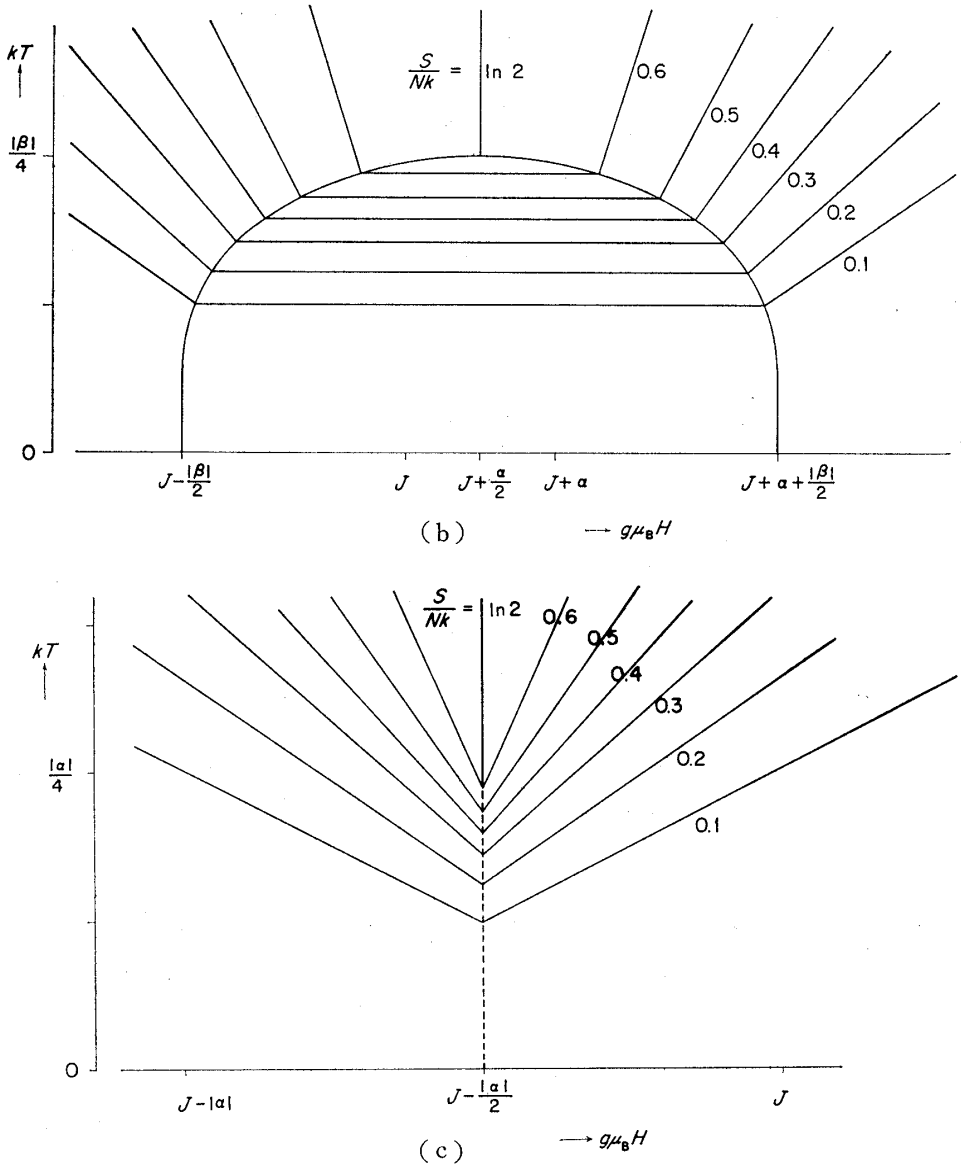

Fig. 7. The contour lines of constant entropy in the H-T plane.
(a) Case *a*. The lines with arrows indicate the temperature in adiabatic magnetization and demagnetization processes.
(b) Case *b*, (c) Case *c*.

The experimental curves of $Cu(NO_3)_2 2.5H_2O$ presented in Fig. 1 may correspond to the curves in Fig. 7(b), if this substance has a long range order of spin pairs.

The specific heat C_H in the case of $\alpha = |\beta|/2$ is obtained as a function of H and T. The result is illustrated stereographically in Fig. 8. The values of C_H in the case of $\alpha = 0$ is presented in Fig. 11 for a purpose of comparison with the specific heat of one-dimensional lattice of spin-pairs.

Downloaded from https://academic.oup.com/ptps/article/doi/10.1143/PTPS.46.291/1875345 by guest on 20 August 2022

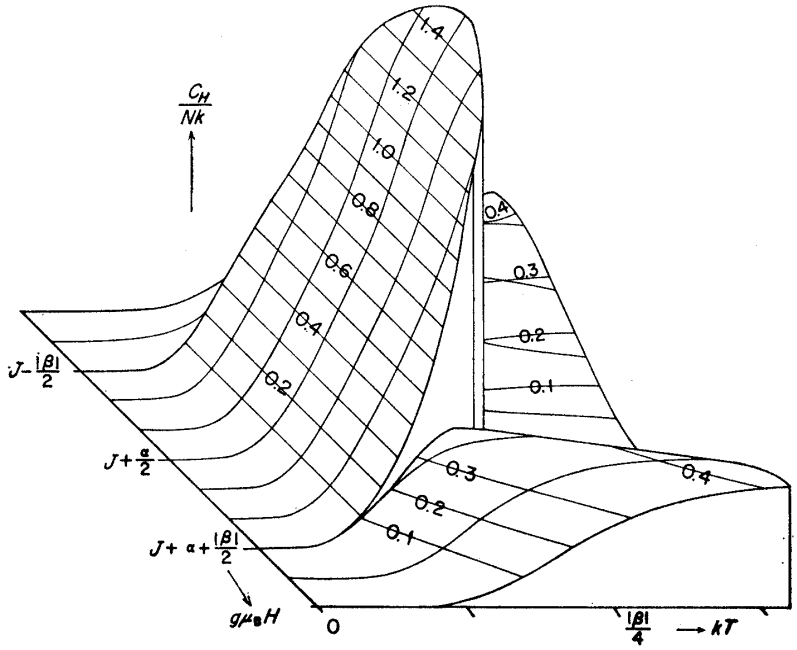

Fig. 8. Stereographic view of the specific heat in the case of $\alpha=|\beta|/2$.

§5. Specific heat of spins in one dimensional lattice

Bonner et al.[7] have proposed two models for the spin array in $Cu(NO_3)_2 \cdot 2.5H_2O$. In one of the models, the pair links form horizontal rungs on a vertical ladder, as shown in Fig. 9(a). Hereafter this is referred to as Model A. In the other the pairs are linked in chains with alternate weak links, as shown in Fig. 9(b). This is referred to as Model B. In these systems no long range order of spins occurs, because the arrays of the spin-pairs are one dimensional. In this section we calculate the specific heat originating from the short range order of spins in the one-dimensional lattices.

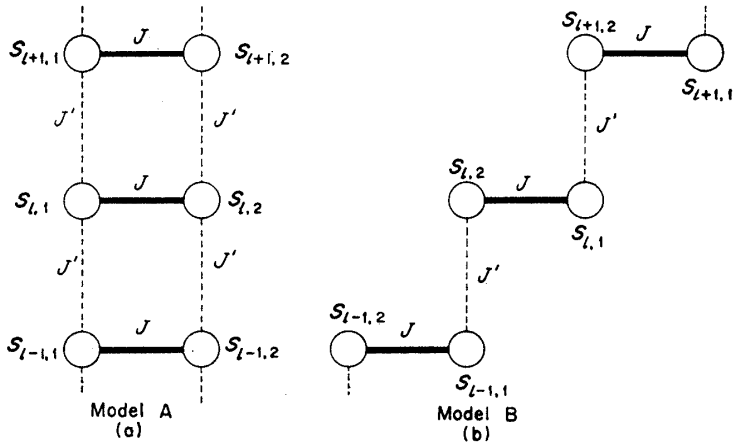

Fig. 9. The two models of the pair-links in $Cu(NO_3)_2\,2.5H_2O$, proposed by Bonner et al.[7] (a) Model A, (b) Model B.

Downloaded from https://academic.oup.com/ptps/article/doi/10.1143/PTPS.46.291/1875345 by guest on 20 August 2022

The Hamiltonian for Model A is written as

$$\mathcal{H}=J\sum_l \boldsymbol{s}_{l1}\cdot\boldsymbol{s}_{l2}+g\mu_B\boldsymbol{H}\cdot\sum_l(\boldsymbol{s}_{l1}+\boldsymbol{s}_{l2}) +J'\sum_l \boldsymbol{s}_{l1}\cdot\boldsymbol{s}_{l+1,1}+J'\sum_l \boldsymbol{s}_{l2}\cdot\boldsymbol{s}_{l+1,2}\,. \tag{65}$$

If we confine ourselves to the lowest two-dimensional subspace of the pair in the same way as in §2, the Hamiltonian is expressed by using the relations (3) and (6) as

$$\begin{aligned}\mathcal{H}=&(N/2)\{J+(J'/4)-g\mu_B H\}\\ &+(1/2)\{g\mu_B H-J-(J'/2)\}\sum_l\sigma_{zl}\\ &+(J'/8)\sum_l\{2(\sigma_{xl}\sigma_{x,l+1}+\sigma_{yl}\sigma_{y,l+1})+\sigma_{zl}\sigma_{z,l+1}\}\,.\end{aligned} \tag{66}$$

The Hamiltonian for Model B is written as

$$\mathcal{H}=J\sum_l \boldsymbol{s}_{l1}\cdot\boldsymbol{s}_{l2}+g\mu_B\boldsymbol{H}\cdot\sum_l(\boldsymbol{s}_{l1}+\boldsymbol{s}_{l2})+J'\sum_l \boldsymbol{s}_{l1}\cdot\boldsymbol{s}_{l+1,2}\,. \tag{67}$$

In the lowest two-dimensional subspace, the Hamiltonian is exprssed as

$$\begin{aligned}\mathcal{H}=&(N/2)\{J+(J'/8)-g\mu_B H\}\\ &+(1/2)\{g\mu_B H-J-(J'/4)\}\sum_l\sigma_{zl}\\ &-(J'/16)\sum_l\{2(\sigma_{xl}\sigma_{x,l+1}+\sigma_{yl}\sigma_{y,l+1})-\sigma_{zl}\sigma_{z,l+1}\}\,.\end{aligned} \tag{68}$$

It is noticed that the x- and y-components of the exchange interaction in Eqs. (66) and (68) are twice as large as the z-component. Similarly to the case of the long range order discussed in §3, this anisotropic exchange interaction causes the short range order of the spin components perpendicular to the field at sufficiently low temperatures. In order to investigate the qualitative nature of the thermodynamical properties of this system, we can use the XY model instead of Model A and Model B, as discussed in a previous paper.[8] The Hamiltonian in this case is written, apart from the constant term independent of the spin states, as

$$\mathcal{H}=(f/2)\sum_l\sigma_{zl}+K\sum_l(\sigma_{xl}\sigma_{x,l+1}+\sigma_{yl}\sigma_{y,l+1}), \tag{69}$$

where f and K stand for the following quantities

$$\begin{cases} f=g\mu_B H-J-(J'/2), \\ K=J'/4 \qquad \text{in the case of Model A,}\end{cases} \tag{70}$$

$$\begin{cases} f=g\mu_B H-J-(J'/4), \\ K=-J'/8 \qquad \text{in the case of Model B.}\end{cases} \tag{71}$$

According to Katsura,[9] the free energy of this system is given by

Downloaded from https://academic.oup.com/ptps/article/doi/10.1143/PTPS.46.291/1875345 by guest on 20 August 2022

$$F=-(NkT/\pi)\int_0^{\pi}\ln\left[2\cosh\{(f-4K\cos\omega)/(2kT)\}\right]d\omega. \qquad (72)$$

By using the free energy, the specific heat is obtained as

$$C_H=(Nk/\pi)\int_0^{\pi}\left[\{(f-4K\cos\omega)/(2kT)\}^2\right.$$
$$\left.\times\operatorname{sech}^2\{(f-4K\cos\omega)/(2kT)\}\right]d\omega. \qquad (73)$$

Integrating numerically Eq. (73), we obtain the temperature dependence of the specific heat for several values of the effective field. The results are shown in Fig. 10(a) and (b). In Fig. 10(a), the broad peaks of the curves for fields $f/4K>1$ correspond to Schottky anomalies associated with the Zeeman levels in the effective field f. The temperature of the peak increases with increasing effective field. On the other hand, the peak at $kT/2K=0.65$ when $f=0$ originates from the short range order of spins and the temperature of the peak decreases as the effective field increases. The details of this behavior are shown in Fig. 10(b). Shoulders in the specific heat curves in this figure originate from the short range order of spins and the shoulder shifts to the low temperature side as the effective field increases.

For the sake of comparison, we calculated the specific heat coming from the long range order of spins in the XY model by using a molecular field approximation. The result is shown in Fig. 11. There is a sharp peak of the specific heat at the critical temperature which decreases as the effective field increases. Since the temperature and field dependences of the specific

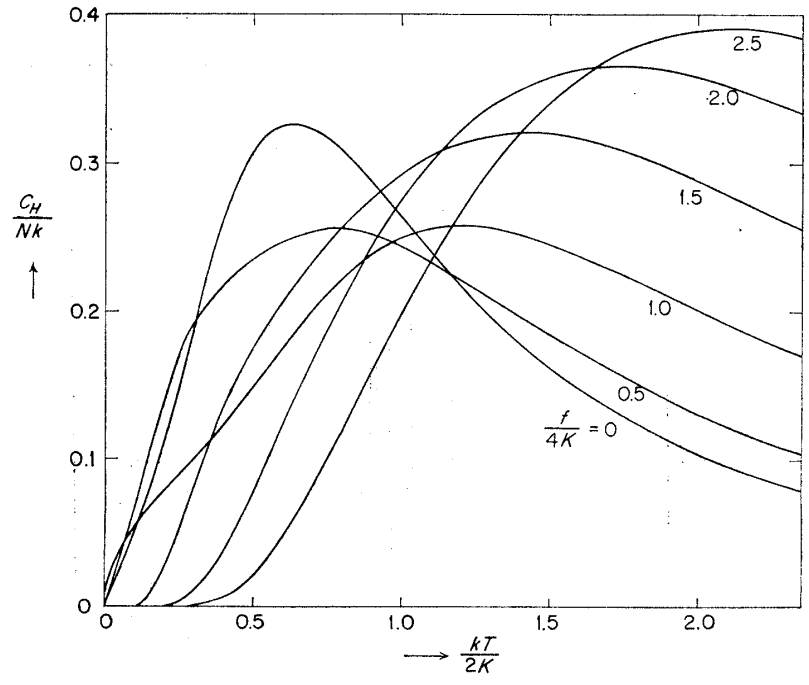

(a)

Downloaded from https://academic.oup.com/ptps/article/doi/10.1143/PTPS.46.291/1875345 by guest on 20 August 2022

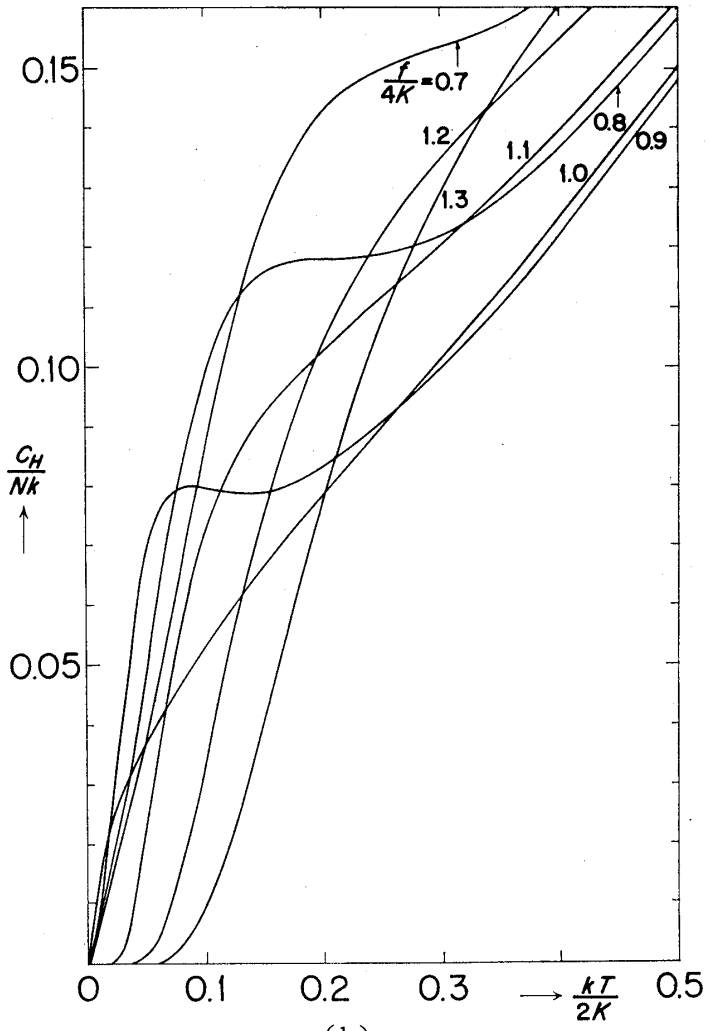

(b)

Fig. 10. The temperature dependence of the specific heat of spins for several values of f in the one-dimensional XY model.

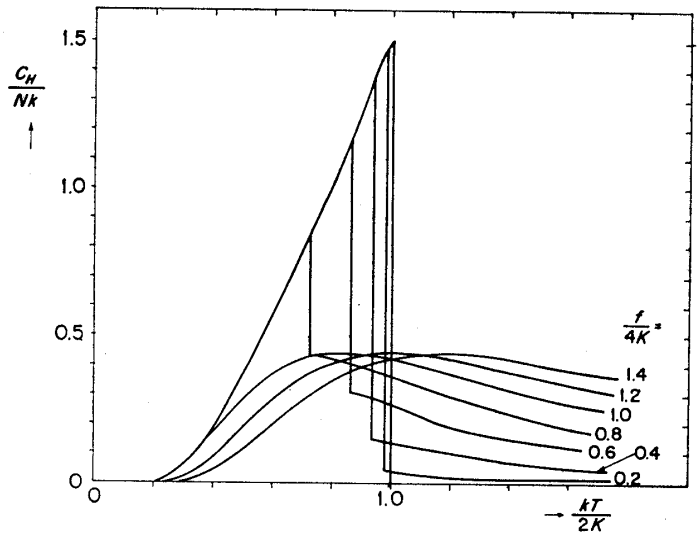

Fig. 11. The temperature dependence of the specific heat of spins for several values of f in the three-dimensional XY model.

Downloaded from https://academic.oup.com/ptps/article/doi/10.1143/PTPS.46.291/1875345 by guest on 20 August 2022

heat in Fig. 10 are very different from those in Fig. 11, measurements of the specific heat of $Cu(NO_3)_2 2.5 H_2O$ may determine whether the anomaly observed by Haseda et al. originate from the short range order of spins or from the long range order of spins.

Acknowledgment

The numerical computation of the specific heat presented in Fig. 10 was made by Mr. E. Tamakawa and Mr. S. Maekawa.

References

1) L. Berger, S. A. Friedberg and J. T. Schriempf, Phys. Rev. **132** (1963), 1057.
2) B. E. Myers, L. Berger and S. A. Friedberg, J. Appl. Phys. **40** (1969), 1149.
3) S. A. Friedberg and C. A. Raquet, J. Appl. Phys. **39** (1968), 1132.
4) T. Haseda, Y. Tokunaga, Y. Kuramitsu, K. Amaya and S. Sakatsume, to be published in *Proceedings of the Twelfth International Conference on Low Temperature Physics, Kyoto* (1970).
5) M. Tachiki and T. Yamada, J. Phys. Soc. Japan **28** (1970), 1413.
6) M. Tachiki, T. Yamada and S. Maekawa, J. Phys. Soc. Japan **29** (1970), 656.
7) J. C. Bonner, S. A. Friedberg, H. Kobayashi and B. E. Myers, to be published in *Proceedings of the Twelfth International Conference on Low Temperature Physics, Kyoto* (1970).
8) M. Tachiki, T. Yamada and S. Maekawa, J. Phys. Soc. Japan **29** (1970), 663.
9) S. Katsura, Phys. Rev. **127** (1962), 1508; **129** (1963), 2835.

Downloaded from https://academic.oup.com/ptps/article/doi/10.1143/PTPS.46.291/1875345 by guest on 20 August 2022